New toxins homologous to ParE belonging to 3-component toxin-antitoxin systems in Escherichia coli O157:H7

Régis Hallez, Damien Geeraerts, Yaan Sterckx, Natacha Mine, Remy Loris, Laurence van Melderen

molecular microbiology

New toxins homologous to ParE belonging to 3-component toxin-antitoxin systems in Escherichia coli O157:H7

Journal:	*Molecular Microbiology*
Manuscript ID:	MMI-2009-08548.R3
Manuscript Type:	Research Article
Date Submitted by the Author:	09-Mar-2010
Complete List of Authors:	hallez, régis; fundp, URBM Geeraerts, Damien; Université Libre de Bruxelles, Laboratoire de Génétique et physiologie bactérienne sterckx, Yaan; VUB, Structural iolgy Mine, Natacha; ULB, Génétique et physiologie Bactérienne Loris, Remy; VUB, Structural iolgy Van Melderen, Laurence; Université Libre de Bruxelles, Laboratoire de Génétique et physiologie bactérienne
Key Words:	Bactericidal toxins, ParE localization

New toxins homologous to ParE belonging to 3-component toxin-antitoxin systems in *Escherichia coli* O157:H7

Régis Hallez [1, ¶], Damien Geeraerts [1], Yann Sterckx [2, 3], Natacha Mine [1], Remy Loris [2, 3] and Laurence Van Melderen [1, *]

[1] Laboratoire de Génétique et Physiologie Bactérienne, Institut de Biologie et de Médecine Moléculaires (IBMM), Faculté des Sciences, Université Libre de Bruxelles, 12, rue des Professeurs Jeener et Brachet, B-6041 Gosselies, Belgium

[2] Structural Biology Brussels, Vrije Universiteit Brussel, Pleinlaan 2, 1050 Brussels, Belgium

[3] Structural Biology Brussels, Department of Molecular and Cellular Interactions, VIB, Pleinlaan 2, 1050 Brussels, Belgium

[*] Corresponding author: E-mail: lvmelder@ulb.ac.be

Phone: +32 2 650 97 78

Fax: +32 2 650 97 70

[¶] Present address: Unité de Recherche en Biologie Moléculaire (URBM), Facultés Universitaires Notre-Dame de la Paix (FUNDP), Rue de Bruxelles 61, B-5000 Namur, Belgium

Running title: New antitoxin and transcriptional regulator associated with ParE

Keywords: Bactericidal toxins, ParE localization

Character count including spaces: 55.701

ABSTRACT

Type II toxin-antitoxin (TA) systems are considered as protein pairs in which a specific toxin is associated with a specific antitoxin. We have identified a novel antitoxin family (*paaA*) that is associated with *parE* toxins. The *paaA-parE* gene pairs form an operon with a third component (*paaR*) encoding a transcriptional regulator. Two paralogous *paaR-paaA-parE* systems are found in *E. coli* O157:H7. Deletions of the *paaA-parE* pairs in O157:H7 allowed us to show that these systems are expressed in their natural host and that PaaA antitoxins specifically counteract toxicity of their associated ParE toxin. For the *paaR2-paaA2-parE2* system, PaaR2 and Paa2-ParE2 complex are able to regulate the operon expression and both are necessary to ensure complete repression. The *paaR2-paaA2-parE2* system mediates ClpXP-dependent post-segregational killing. The PaaR2 regulator appears to be essential for this function, most likely by maintaining an appropriate antitoxin:toxin ratio in steady-state conditions. Ectopic overexpression of ParE2 is bactericidal and is not resuscitated by PaaA2 expression. ParE2 co-localizes with the nucleoid, while it is diffusely distributed in the cytoplasm when PaaA2 is co-expressed. This indicates that ParE2 interacts with DNA-gyrase cycling on DNA and that co-expression of PaaA2 antitoxin sequesters ParE2 away from its target by protein-protein complex formation.

INTRODUCTION

Type II toxin-antitoxin (TA) systems are generally composed of two small open reading frames (ORFs) organized in an operon in which the antitoxin gene is located upstream of the toxin gene (Gerdes *et al.*, 2005). The toxins characterized so far appear to interefere either with DNA replication or translation. On the one hand, toxins such as CcdB and ParE poison DNA-gyrase, which is an essential toposiomerase II in *Escherichia coli* (Bernard & Couturier, 1992, Bernard *et al.*, 1993, Jiang *et al.*, 2002). Interaction of CcdB with its target results in severe inhibition of replication and transcription, SOS induction and drastic reduction of viability (for review (Van Melderen, 2002)). On the other hand, toxins such as RelE, MazE and HipA inhibit translation through various mechanisms (cleavage of mRNAs, naked or associated with the ribosomes, phosphorylation of EF-TU). These toxins inhibit cell growth in a reversible manner (Christensen *et al.*, 2004, Pedersen *et al.*, 2003, Suzuki *et al.*, 2005, Liu *et al.*, 2008, Schumacher *et al.*, 2009, Winther & Gerdes, 2009). Antitoxins neutralize toxins through direct protein-protein interactions and have also the ability to bind, either alone or in complex with their cognate toxin, to the TA promoter region to repress expression of the operon. Autoregulation appears to be essential for avoiding overexpression of the TA components in steady-state conditions (e.g. Afif *et al.*, 2001, Magnuson & Yarmolinsky, 1998, Monti *et al.*, 2007). Antitoxin proteins are degraded by ATP-dependent proteases, which results in a shorter half-life than that of the toxin protein (Gerdes et al., 2005). Antitoxin instability constitutes the molecular basis of the post-segregational killing (PSK) phenomenon by which plasmid-encoded TA systems secure plasmid maintenance. Indeed, the relative antitoxin instability forces the bacterial host to maintain a constant production of the antitoxin to avoid growth arrest or killing, depending on the nature of the toxin. For example, the bacteriosatic toxin Kid (R1 plasmid) will arrest bacterial growth (Jensen *et al.*, 1995) while the bactericidal toxin CcdB (F plasmid) will kill the cell by poisoning the DNA-gyrase (Bernard &

Couturier, 1992, Bernard et al., 1993). Upon plasmid loss, the newborn plasmid-free cells will no longer produce antitoxin and toxin proteins. Since the antitoxin is degraded, the toxin will be free to act on its target and interfere with essential cellular processes. Thus, plasmid-encoded TA systems participate in plasmid maintenance in growing populations by selectively inhibiting growth or killing plasmid-free progenies (Gerdes *et al.*, 1986, Jensen et al., 1995). Bioinformatics searches reavealed that bacterial chromosomes contain a large number of TA systems, sometimes in an impressive number (*e.g.* more than 45 different TA loci in *Photorabdus luminescens*) (Fozo *et al.,* 2010*,* Jorgensen *et al.*, 2009, Makarova *et al.*, 2009, Pandey & Gerdes, 2005, Sevin & Barloy-Hubler, 2007).

The biological roles of these chromosomally-encoded TA systems are still under debate and might differ depending notably on the bacterial species, localization (mobile genetic element or chromosomal backbone), or type of toxin (bacteriostatic or bactericidal) (for reviews (Magnuson, 2007, Van Melderen & Saavedra De Bast, 2009)).

Previously, 3 paralogous *parE* toxin genes encoded in the *E. coli* O157:H7 chromosome were described as being part of 3 *parDE* TA systems (Pandey & Gerdes, 2005). Here, we show that 2 of these 3 *parE* toxins are indeed associated with a new familly of antitoxins devoid of predicted DNA-binding domain. Autoregulation is ensured by the antitoxin-toxin complex and by a separate transcriptional regulator encoded by an upstream gene within the same operon. Moreover, this regulator is essential to maintain an appropriate antitoxin:toxin ratio. We also show here that the ParE toxin is bactericidal and co-localizes with the bacterial nucleoid.

RESULTS

The chromosomal parE homologs of E. coli O157:H7 are associated with small hypothetical ORFs

Three *parE* homologs were previously detected in the chromosome of the enterohemorrhagic *E. coli* O157:H7 (Pandey & Gerdes, 2005). These 3 ParE proteins contain the COG3668 domain related to ParE and share about 24% of identity with the canonical ParE toxin from the broad-host range RK2 plasmid (Table S1). Although these *parE* homologs (*parE1*: NP_309094, *parE2*: NP_310308 and *parE3*: NP_308489) have been considered as being part of 3 canonical *parDE* systems (Pandey & Gerdes, 2005), a *parD* homolog was detected only upstream of *parE3*. This ORF (NP_308488) encodes a protein sharing 20% of identity with the canonical $ParD_{RK2}$ antitoxin (Table S1). It contains a predicted DNA-binding domain (DNA-BD) belonging to the RHH2 family (pfam03693) which is related to the CopG/Arc/Met domain (COG3609) found in $ParD_{RK2}$. The ORF NP_308488 was therefore named $parD_{EDL933}$ (Figure 1). The ORFs located upstream of the *parE1* and *parE2* genes (NP_309095 and NP_310307) encode small hypothetical proteins which share virtually no identity with the canonical $ParD_{RK2}$ antitoxin (5% and 12% respectively, Table S1). These hypothetical proteins are devoid of known DNA-BD. Interestingly, the ORFs located upstream of NP_309095 and NP_310307 (NP_309096 and NP_310306, respectively) encode putative transcriptional regulators containing a DNA-BD of the DicA transcriptional repressor family (PRK09706; (Cam *et al.*, 1988)). This might indicate a new type of toxin-antitoxin locus composed of a *parE* toxin-encoding gene associated with a novel antitoxin gene and a novel transcriptional repressor. The ORFs NP_309095 and NP_310307 encoding the putative novel antitoxins were respectively named *paaA1* and *paaA2* (for *parE*-associated antitoxin), and the ORFs NP_309096 and NP_310306 were renamed *paaR1* and *paaR2* (for *parE*-associated transcriptional repressor), respectively.

The chromosomal parE homologs encode toxic proteins inducing the SOS response

To test whether the 3 chromosomally-encoded *parE* homologs encode toxic proteins, viability of *E. coli* MG1655 strain overexpressing the 3 *parE* genes of O157:H7 as well as the $parE_{RK2}$ of the RK2 plasmid was measured. Overexpression of the *parE* genes dramatically reduced MG1655 viability, with a 10^4-fold reduction for *parE1*, *parE2* and $parE_{RK2}$, and a 10^2-fold reduction for *parE3*, after 90 minutes of induction (Figure S1A). Microscope examinations revealed that overexpression of the 4 *parE* genes strongly induced filamentation, although to a lesser extent for *parE3* (data not shown). Ability of ParE1, ParE2, ParE3 and $ParE_{RK2}$ to induce the SOS system was tested using a λ*sfiA::lacZ* fusion. The pBAD33-$ccdB_F$ plasmid was used as a positive control for SOS induction. $CcdB_F$ as well as the 4 ParE toxins strongly induced *sfiA::lacZ* activity although to a lesser extent for *parE3* (Figure S1B), which is in good agreement with viability loss and filamentation data. These data show that the 3 ParE homologs encoded in O157:H7 chromosome are active toxins that induce the SOS system, most likely by inhibiting DNA-gyrase activity.

The ORFs located upstream of the parE genes encode functional antitoxins specific to their associated toxins

To test whether the genes located upstream of the *parE* paralogs encode functional antitoxins, *paaA1*, *paaA2*, $parD_{EDL933}$ and $parD_{RK2}$ (as a positive control) were cloned in the pKK223-3 expression vector under the P*tac* promoter control. The *E. coli* DJ624 ($lacI^Q$) strain harbouring pKK223-3 derivative plasmids and compatible *parE*-containing pBAD33 plasmids were tested on plates supplemented either with glucose (to repress pBAD promoter) or with arabinose and IPTG (to simultaneously induce pBAD and P*tac* promoters). The strains harbouring pKK223-3 vector with one of the *parE*-containing pBAD33 plasmids (Figure 2A2, first column) were not able to form colonies on arabinose/IPTG-containing plates, confirming that expression *parE1*, *parE2*, *parE3* and

parE$_{RK2}$ is toxic for *E. coli*. On the contrary, strains coexpressing one of the *parE* genes with its cognate antitoxin gene (*parE1*/*paaA1*, *parE2*/*paaA2*, *parE3*/*parD*$_{EDL933}$) as well as the positive control *parE*$_{RK2}$/*parD*$_{RK2}$ were able to grow on arabinose/IPTG-containing plates (Figure 2A2, diagonal). The strains harbouring pBAD33 with one of the pKK223-3 derivative plasmids (Figure 2A2, first line) were able to grow on arabinose/IPTG-containing plates, indicating that expression *paaA1*, *paaA2*, *parD*$_{EDL933}$ and *parD*$_{RK2}$ is not toxic for *E. coli*. These results showed that *paaA1*, *paaA2* and *parD*$_{EDL933}$ encode functional antitoxins. These antitoxins specifically counteract the toxicity of their cognate ParE toxins since no cross-talk between toxins and antitoxins was observed. This last result was unexpected for the paralogous *paaA* genes since both antitoxins (PaaA1 and PaaA2) and toxins (ParE1 and ParE2) share more than 60% of identity (Table S1).

The experiments presented above were performed in MG1655, which do not encode the *parE* loci in their genome. To characterize the *parE* loci in their natural host, the *E. coli* O157:H7 EDL933 strain was transformed with the *parE*-containing pBAD33 plasmids. The resulting transformants were streaked on plates supplemented with either glucose or arabinose. While overexpression of *parE*$_{RK2}$ inhibited colony formation on arabinose-containing plates (Figure 2B2, 4th line), none of the chromosomal *parE* genes overexpressed from a pBAD plasmid inhibited growth of O157:H7. This indicates that *paaA1*, *paaA2* and *parD*$_{EDL933}$ are expressed in O157:H7 at a level sufficient to counteract the toxicity of their cognate ParE toxins produced *in trans*. To test this, the antitoxin-toxin gene pairs were deleted, and the resulting mutant strains (Δ*paaA1-parE1::kan*, Δ*paaA2-parE2::kan* and Δ*parD*$_{EDL933}$*-parE3::kan*) were transformed with the *parE*-expressing pBAD33 plasmids. The resulting transformants were tested on plates supplemented with glucose or arabinose (Figure 2B). Overexpression of *parE1*, *parE2* and *parE3* led to growth inhibition of the mutant deleted of the cognate TA system (Figure 2B2, diagonal), *e.g. parE2* only inhibited growth of Δ*paaA2-parE2::kan*. These results confirm that PaaA1, PaaA2 and ParD$_{EDL933}$ antitoxins specifically counteract their

cognate toxins. Altogether, these results show that the PaaA proteins constitute a novel family of antitoxins associated with ParE-like toxins.

Ectopic overexpression of ParE2 is bactericidal

Most of the TA systems described so far encode bacteriostatic toxins inhibiting translation and therefore arresting cell growth. Antitoxins associated with these bacteriostatic toxins can relieve toxicity and resuscitate inhibited cells even after a prolonged exposure to the toxin (Pedersen et al., 2003). In contrast, ParE and CcdB toxin families are tought to be bactericidal since interactions with DNA-gyrase leads to major damages (double-strand DNA breaks) (Bernard et al., 1993, Jiang et al., 2002, Critchlow *et al.*, 1997). To test whether the effect of ectopic overexpression of ParE is reversible, PaaA2 overexpression was induced subsequently to that of ParE2 in the DJ624 *Δara*/pBAD-*parE2*/p*lac*-*paaA2* strain. Strain was grown in liquid media containing arabinose with or without IPTG. Samples were plated on plates containing glucose with or without IPTG (Figure 3). Growth was comparable to that of DJ624 *Δara* harbouring control plasmids (open circles), with a 10^2-fold increase of CFU after 150 minutes of *parE2* expression in the presence of IPTG in the liquid culture and on plates (filled square and black line). Thus, this confirms that continous expression of PaaA2 antagonises ParE2 toxicity. When *paaA2* was not expressed on plates (filled square and dotted line), normal growth was observed for 60 min of *parE2* expression. After 90 min, viable counts drastically decreased with a 10^4-fold reduction.

When *paa2* was not expressed in the liquid culture (open squares), a 10^3-fold reduction in viability was observed after 60 min of *parE2* expression (open squares and dotted line) and is comparable to viability loss observed when *paaA2* is expressed on plates (open square and black line). Thus, accumulation of DNA damages during 30 min of ParE2 overexpression is sufficient to cause drastic

loss of viability, whether or not PaaA2 is subsequently expressed, showing that ectopic overexpression of ParE2 is bactericidal.

ParE2 localizes over the nucleoid and PaaA2 prevents this localization through a physical interaction

To further characterize the PaaA antitoxin family, the ability of PaaA2 to interact with ParE2 was tested. Co-immunoprecipitation (Co-IP) assays were performed using anti-FLAG antibodies and cell lysates of MG1655 expressing *paaA2-flag* from the P*tac* promoter and either *parE2-gfp* or *gfp* alone from the pBAD promoter. ParE2-GFP and PaaA2-FLAG fusions were shown to be functional (*i.e.* ParE2-GFP as toxic as the untagged ParE2 toxin and counteracted by its specific untagged antitoxin PaaA2 or PaaA2-FLAG, data not shown). These Co-IP experiments revealed that ParE2-GFP is specifically pulled down by PaaA2-FLAG (Figure 4A, IP). This result shows that PaaA2 and ParE2 are part of the same protein complex. Interaction between PaaA2 and ParE2 was confirmed with purified proteins in a gel filtration assay (data not shown).

Localization of ParE2 using the *parE2-gfp* fusion revealed that ParE2-GFP is predominantly found as a patch of fluorescence surrounding the cell center of filamentous cells (Figure 4B). The staining of chromosomal DNA using DAPI showed that ParE2-GFP colocalized with the nucleoid (Figure S2). These results suggest that ParE2 binds its target complexed to DNA, most likely the DNA-gyrase as previously shown *in vitro* (Jiang et al., 2002). Interestingly, co-expression of *paaA2-flag* leads to a complete delocalization (Figure 4C). Similar results were obtained when *flag-paaA2* or the untagged version of *paaA2* was co-expressed (data not shown). *gfp-paaA2* or *paaA2-gfp* fusions expressed from a pBAD promoter produce a diffuse signal in the cytoplasm (Figure 4D), showing that PaaA2 does not localize on the nucleoid. These data suggest that in co-expression conditions, PaaA2 and ParE2 form a cytoplasmic complex that prevents ParE2 to localize over the nucleoid.

PaaR2 and the PaaA2-ParE2 TA complex repress the expression of the 3-component paaR2-paaA2-parE2 system

Short intergenic regions between the genes of the *paaR2-paaA2-parE2* system (Figure 1) suggest a polycistronic organization. RT-PCR experiments showed that *paaR2-paaA2-parE2* is indeed expressed as a tri-cistronic mRNA (data not shown). A σ^{70}-dependent promoter was predicted upstream of the *paaR2* gene, likely driving the expression of the locus (Figure 5A). This predicted promoter was fused to *lacZ* (P*R2-lacZ*) and β-galactosidase activity was assayed in *E. coli* strains overexpressing various combinations of the 3 components *in trans* (Figure 5B). The P*R2-lacZ* fusion yielded 146 ± 5 Miller units, indicating that a weak promoter lies within the 100 bp fragment upstream of *paaR2* (Figure 5B). On the one hand, expression of *paaR2* by itself or in combination with *paaA2-parE2* led to a drastic reduction in the β-galactosidase activity of P*R2-lacZ*, showing that PaaR2 is a transcriptional repressor. On the other hand, expression of *paaA2-parE2* decreased the activity of P*R2-lacZ* of more than 40% (84 ± 7 Miller units). Expression of *paaA2* by itself did not reduce the β-galactosidase activity of the P*R2-lacZ* (168 ± 4 Miller units) (Figure 5B). This shows that the PaaA2-ParE2 complex is able to repress the P*R2* promoter.

The above experiments were performed in overexpression conditions. To avoid a possible effect, autoregulation was tested *in cis* (*i.e.* expressed directly from the P*R2* promoter), with or without the toxin and antitoxin components. Transcriptional fusions with *lacZ* fused downstream of *paaR2*, *paaR2-paaA2* or *paaR2-paaA2-parE2* were constructed (P*R2-paaR2-lacZ*, P*R2-paaR2-paaA2-lacZ* and P*R2-paaR2-paaA2-parE2-lacZ*) and assayed for β-galactosidase activity. The presence of *paaR2* alone or with *paaA2* decreased the LacZ activity of about 40% (42% and 48% respectively) while the P*R2-paaR2-paaA2-parE2-lacZ* fusion had no detectable LacZ activity (Figure 5C). This was not

caused by the presence of a transcription terminator downstream of *paaR2* since an in-frame deletion of *paaR2* (giving rise to the P*R2-paaA2-parE2-lacZ* fusion) restored LacZ activity (data not shown). These data show that the presence of the 3 components (PaaR2, PaaA2 and ParE2) is necessary to achieve complete repression of the P*R2* promoter. However, we were unable to detect a 3 protein-complex in the conditions we tested (data not shown), indicating that the 2 repressor complexes may act independently.

Chromosomal TA systems have been proposed to be stress response modules. We tested the transcriptional activity of the P*R2-paaR2-paaA2-parE2-lacZ* fusion under several stress conditions known to activate notably the *E. coli mazEF* system (42°C, rifampicin (10µg/ml), SHT (2.5mg/ml), Mitomycin C (2µg/ml) (Christensen *et al.*, 2003, Sat *et al.*, 2001). None of these conditions induced the P*R2* promoter (data not shown).

The paaR2-paaA2-parE2 system of E. coli O157:H7 is able to mediate ClpAP- and ClpXP-dependent post-segregational killing

Analysis of the *paaR2-paaA2-parE2* neighbouring genes as well as prediction of prophage content using the Prophinder website (Lima-Mendez *et al.*, 2008) indicated that this TA system is located in a prophage (prophinder: 43332). This system might participate to prophage stabilization as it has been shown for TA systems located in some genomic islands (Budde *et al.*, 2007, Christensen-Dalsgaard & Gerdes, 2006, Rowe-Magnus *et al.*, 2003, Szekeres *et al.*, 2007, Wozniak & Waldor, 2009). The pMLO-*paaR2-paaA2-parE2* plasmid was constructed to test whether this TA system is able to mediate post-segregational killing (PSK). As shown in Figure 6 and Figure S3A, after 180 minutes at non-permissive temperature (42°C), the ability of MG1655 harbouring the pMLO-*paaR2-paaA2-parE2* plasmid to form colonies decreased of 74% as compared to the control MG1655/pMLO59. The plasmid titer did not increase after 90 minutes at 42°C (Figure S3A),

showing that the pMLO-*paaR2-paaA2-parE2*-dependent toxic effect is post-segregational. Moreover, microscope examinations of MG1655 harbouring the pMLO-*paaR2-paaA2-parE2* plasmid showed a high number of filamentous bacteria at restrictive temperature (data not shown). Viability of the *clpP::cat*, the *clpA::kan* and *clpX::kan* mutants was similar to that of MG1655/pMLO59 (114%, 85% and 85% respectively, Figure 6), showing that PSK mediated by the *paaR2-paaA2-parE2* system was abolished in these mutants (Figure S3A). These results suggest that ClpAP and ClpXP proteases are responsible for PaaA2 degradation. The *lon::tet* mutant showed an increased sensitivity to the *paaR2-paaA2-parE2*-dependent PSK (Figure S3A and Figure 6). Lon mutants are particularly sensitive to SOS induction due to accumulation of the SfiA division inhibitor, which is a Lon substrate.

To test whether PaaR2 is necessary for PSK, *paaR2* was deleted and the resulting pMLO-*paaA2-parE2* plasmid was tested for its ability to mediate PSK. Surprisingly, MG1655/pMLO-*paaA2-parE2* displayed a 10^2-fold reduction in viability in comparison to MG1655/pMLO-*paaR2-paaA2-parE2* after 180 minutes at 42°C (Figure 6). The pMLO-*paaA2-parE2* plasmid titer was lower than that observed for the complete system at 42°C (< 0.01% as compared to ~ 2%), showing that the pMLO-*paaA2-parE2*-dependent killing effect is independent of plasmid loss (Figure S3B and Figure 6). This unstable behaviour was neutralized in the wild-type strain expressing *paaA2 in trans* (Figure S3B and Figure 6). These data indicate that *paaR2* is crucial for maintaining an appropriate antitoxin:toxin ratio and therefore to ensure viability in steady-state conditions.

PaaA2 is an unstable protein hierachically degraded by several proteases in vivo

Previous experiments strongly suggest that PaaA2 is unstable. Using pulse-chase experiments, PaaA2 was found to be unstable in MG1655 with a half-life shorter than 20 min (data not shown). In agreement with the radioactive labeling experiments performed with the untagged PaaA2 protein, we

found that PaaA2-FLAG had a half-life of about 6 min in the wild-type strain as well as in the *lon::tet* and *clpA::kan* mutants (Table 1). The half-life of PaaA2-FLAG was slightly increased ($t_{1/2}$ ~10 min) in the *clpX::kan* mutant and further increase was observed in a *clpP::cat* mutant ($t_{1/2}$ ~ 30 min) and *clpX::kan clpA::tet* ($t_{1/2}$ ~50 min). Paa2-FLAG was completely stabilized in a *Δlon clpP::cat* mutant ($t_{1/2}$ > 120 min). This shows that PaaA2 is unstable and hierarchically degraded by ClpXP, ClpAP and Lon.

DISCUSSION

Classification of type II TA systems is based on similarities of toxin protein sequences. Ten canonical type II families are desribed so far, in which a specific antitoxin is assigned to a specific toxin (*relBE*, *mazEF*, *vapBC*, *phd-doc*, *ccd*, *parDE*, *higBA*, *hipAB*, *hicAB* and ω–ε–ζ) (Jorgensen et al., 2009, Gerdes et al., 2005). As an exemple, the *parDE* toxin-antitoxin system family is composed of the *parE* toxin gene specifically associated to the *parD* antitoxin gene (Gerdes et al., 2005). Few exceptions to this rule have been published recently, notably the *prlF-yhaV* system of *E. coli* in which the *prlF* antitoxin is a *mazE* homologue and the *yhaV* toxin is homologous to *relE*, both belonging to disctinct families according to current classification (Schmidt *et al.*, 2007). Here, we described a new antitoxin gene family (*paaA*) associated with *parE*, showing that at least two different antitoxin types are associated with the *parE* toxin gene family. Two systems of this type are found in the *E. coli* O157:H7 genome and co-exist independently since the PaaA1 antitoxin is unable to counteract ParE2 toxicity and vice-versa.

We identified a third gene, *paaR*, which is part of the *paaA-parE* operons and located upstream of *paaA* genes. Several attempts to construct a deletion of the *paaR2* gene in *E. coli* O157:H7 were unsuccessful (data not shown), suggesting that PaaR2 might play a major regulatory role for *paaA2-parE2* expression. Indeed, we have shown that PaaR2 represses *paaA2-parE2* expression both in *trans* and *cis*. Interestingly, the PaaA2-ParE2 complex also regulates negatively *paaA2-parE2* expression. Complete repression requires both PaaR2 and PaaA2-ParE2 complex, indicating that the *paaR2-paaA2-parE2* locus constitutes a 3-component TA system. Our PSK experiments show indeed that *paaR2* is essential for the maintenance of the *paaR2-paaA2-parE2* system. The reason of this dual control of *paaR2-paaA2-parE2* expression is currently under investigation in our lab. Stress conditions did not alleviate repression of the *paaR2-paaA2-parE2* system, ruling out its implication in stress response.

As far as we know, 3-component TA systems do not appear to be widely distributed in bacteria. Very few examples are reported in the literature and concern the *pasABC* and the ω–ε–ζ systems (Smith & Rawlings, 1997, Ceglowski *et al.*, 1993, de la Hoz *et al.*, 2000, de la Hoz *et al.*, 2004, Dmowski *et al.*, 2006, Weihofen *et al.*, 2006, Zielenkiewicz & Ceglowski, 2005). Functional organization of the ω–ε–ζ system resembles that of *paaR2-paaA2-parE2*, transcriptional regulation being ensured by ω and antitoxicity by ε.

This work also provided new insights regarding mode of action of the ParE toxin. The group of Helinski showed that loss of a plasmid containing the $parDE_{RK2}$ system induces filamentation (Roberts *et al.*, 1994) and that $ParE_{RK2}$ inhibits DNA-gyrase *in vitro* (Jiang et al., 2002). Here, we showed that the overexpression of ParE toxins induce the SOS system, confirming that filamentation previously observed was SOS-dependent. ParE2-GFP co-localizes with the nucleoid, indicating that ParE2 targets DNA-gyrase preferentially when it is cycling on DNA, as shown for CcdB (Bahassi *et al.*, 1999). Co-expression of PaaA2 together with ParE2-GFP completely released the toxin from the nucleoid. Although PaaA2 acts by preventing ParE2-DNA-gyrase interactions, it is not able to resuscitate cells suffering of ParE2 toxicity under overexpression conditions. Thus, neither double-strand breaks repair systems nor PaaA2 antitoxin can rescue DNA damages induced by ParE2 overexpression. This data raises the possibility that ParE is bactericidal in its natural context. Similar results have been obtained with the *ccd* system (Mine and Van Melderen, unpublished results). Antibiotics targeting DNA-gyrase like quinolones are bactericidal, supporting the idea that toxins poisoning DNA-gyrase are bactericidal (Chin & Neu, 1983, Eliopoulos *et al.*, 1985, Hooper, 2001, Zeiler, 1985).

The *paaR2-paaA2-parE2* system is located in a predicted prophage, suggesting that it might participate to prophage stability as shown for TA systems located on mobile genetic elements. Numerous examples are available e.g. *ccd* from the F plasmid and *parDE* from RK2, *relBE* from Qin

prophage in *E. coli* and *mosAT* from the SXT conjugative element of *Vibrio cholerae* (Jaffe *et al.*, 1985, Roberts & Helinski, 1992, Roberts et al., 1994, Gotfredsen & Gerdes, 1998, Wozniak & Waldor, 2009). The *paaR2-paaA2-parE2* system is indeed able to mediate PSK that relies on PaaA2 degradation by several ATP-dependent proteases, preferentially ClpXP. The question of the biological roles of chromosomally-encoded systems remains under debate. This new example reinforces the idea that when located in genomic islands, TA systems participate to stabilization, which is reminiscent to the function they have when located on mobile genetic elements.

EXPERIMENTAL PROCEDURES

Bacterial strains, media and growth conditions

Bacterial strains used in this work are listed in table 2. They are all *E. coli* K-12 derivatives (MG1655 or CSH50) except for O157:H7 EDL933. Strains were routinely grown in LB broth or minimal Ceria medium (MM) (Tsilibaris *et al.*, 2007). Antibiotics were added at the following concentrations when appropriate: kanamycin, 20 µg/ml or 50 µg/ml; chloramphenicol, 20 µg/ml; ampicillin, 100 µg/ml or 500 µg/ml; spectinomycin, 100 µg/ml; tetracycline, 15 µg/ml.

Strains constructions

The *E. coli* O157:H7 EDL933 derivative mutant strains were constructed using the pKOBEG vectors (Chaveroche *et al.*, 2000) as described in (Wilbaux *et al.*, 2007). The kanamycin resistance cassette of pKD4 was amplified by PCR with the following primers: Δ*paaA1parE1* for and Δ*paaA1parE1* rev (strain 133); Δ*paaA2parE2* for and Δ*paaA2parE2* rev (strain 136); Δ*parDparE3* for and Δ*parDparE3* rev (strain 139). Deletions were checked by PCR. The *E. coli* MG1655 *clpX::kan clpA::tet* strain was constructed by transducing *clpA::tet* using a P1 lysate made on MG1655 *clpA::tet* into MG1655 *clpX::kan*.

Plasmids construction

(i) pBAD33-derivative plasmids

The *parE1*, *parE2* and *parE3* coding sequences (CDS) were amplified using *E. coli* O157:H7 EDL933 genomic DNA as template and the following primers: Start-*parE1* and Stop-*parE1*; Start-*parE2* and Stop-*parE2*; Start-*parE3* and Stop-*parE3*. The $parE_{RK2}$ CDS was amplified by PCR using mini-RK2 derivative pMR10 (Mohr and Roberts, unpublished) and the Start-$parE_{RK2}$ and Stop-$parE_{RK2}$ primers. All Start-primers carried a canonical Shine-Dalgarno (SD) sequence. The PCR products were digested with *Xba* I and *Pst* I and ligated into the pBAD33 vector cut with the same

restriction enzymes. The resulting plasmids (pHR033, pHR027, pHR034 and pHR035) were sequenced. The *gfp mut2* CDS was amplified by PCR using the pZD6 plasmid (Ding *et al.*, 2002) as template and the primers *gfp mut2*-T7.tag for and *gfp mut2*-T7.tag rev or T7.tag-*gfp mut2* for and T7.tag-*gfp mut2* rev. The T7.tag-*gfp mut2* PCR product was digested with *Pst* I and *Hin*d III while *gfp mut2*-T7.tag with *Xba* I and *Pst* I. The products were ligated into the pBAD33 vector cut with the same restriction enzymes. The resulting plasmids (pHR054 and pHR055, respectively) were sequenced and used to construct translational fusions to the amino-terminus (pHR054) or the carboxy-terminus (pHR055) of the GFP.

The *parE2* and *paaA2* CDS were amplified on *E. coli* O157:H7 EDL933 genomic DNA using the following primers: Start_RBS-*parE2_Xba* I and Stop'-*parE2_Pst* I; and Start_RBS-*paaA2_Xba* I and Stop'-*paaA2_Pst* I. PCR products were digested with *Xba* I and *Pst* I and ligated into the pHR054 (pBAD33-T7.tag-*gfp mut2*) cut with the same restriction enzymes. The resulting plasmids (pHR119 and pHR073) were sequenced. The *paaA2* CDS was amplified on *E. coli* O157:H7 EDL933 genomic DNA using the primers Start-*paaA2_Pst* I and Stop-*paaA2_Hin*d III. The PCR product was digested with *Pst* I and *Hin*d III and ligated into the pHR055 (pBAD33-*gfp mut2*-T7.tag) cut with the same restriction enzymes. The resulting plasmid (pHR072) was sequenced.

(ii) pKK223-3-derivative plasmids

The *paaA1*, *paaA2* and $parD_{EDL933}$ CDS were amplified using *E. coli O157*:H7 EDL933 genomic DNA as template and the following primers: Start-*paaA1* and Stop-*paaA1*; Start-*paaA2* and Stop-*paaA2*; Start-$parD_{EDL933}$ and Stop-$parD_{EDL933}$. The $parD_{RK2}$ CDS was amplified using mini-RK2 derivative pMR10 as template and the Start-$parD_{RK2}$ and Stop-$parD_{RK2}$ primers. The PCR products were cloned into the TOPO-XL vector (Invitrogen) and sequenced. The recombinant TOPO-XL plasmids were then digested with *Pst* I and *Hin*d III for *paaA1*, and with *Eco* RI and *PstI* for the other CDS. The corresponding DNA fragments were ligated into the pKK223-3 vector opened with

the same restriction enzymes, generating the plasmids pHR036, pHR016, pHR037 and pHR038 respectively.

The *paaR2*, *paaA2-parE2* and *paaR2-paaA2-parE2* DNA fragments were amplified on *E. coli* O157:H7 EDL933 genomic DNA using the following primers: Start-*paaR2_Pst* I and Stop-*paaR2_Hin*d III; Start-*paaR2_Pst* I and Stop-*paaA2*; Start-*paaA2*_RBS *Pst* I and Stop-*parE2_Hin*d III; and Start-*paaR2_Pst*I and Stop-*parE2_Hin*d III. The 4 PCR products were then cut with *Pst* I and *Hin*d III and ligated into the pKK223-3 vector opened with the same restriction enzymes, generating the plasmids pHR082, pHR096, pHR023 and pHR097 respectively.

The *paaA2* CDS was amplified from *E. coli* O157:H7 EDL933 genomic DNA, using the following primers: Start-*paaA2_flag* PstI and Stop-*paaA2_Hin*d III; and Start-*paaA2*_RBS *Pst* I and Stop-*paaA2_flag Hin*d III. Both PCR products were then digested with *Pst* I and *Hin*d III and ligated into the pKK223-3 vector cut with the same restriction enzymes, generating the plasmids pHR117 and pHR122 respectively.

(iii) pWSK129-derivative plasmid

The *paaA2* CDS was amplified on *E. coli* O157:H7 EDL933 genomic DNA using the primers Start_RBS-*paaA2_Xba* I and Stop-*paaA2*. The PCR product was cloned into the TOPO-XL vector (Invitrogen) and sequenced. The recombinant TOPO-XL plasmids was then digested with *Xba* I and *Pst* I and the corresponding DNA fragment was ligated into the pWSK129 vector opened with the same restriction enzymes, generating the plasmid pHR133.

(iv) pJL207-derivative plasmids

The DNA fragments P*R2*, P*R2-paaR2*, P*R2-paaR2-paaA2* and P*R2-paaR2-paaA2-parE2* were amplified on *E. coli* O157:H7 EDL933 genomic DNA using the following primers: P*R2* for and P*R2* rev; P*R2* for and Stop-*paaR2_Hin*d III; P*R2* for and Stop-*paaA2_Hin*d III; P*R2* for and Stop-*parE2_Hin*d III. The PCR products were digested by *Pst* I and *Hin*d III and ligated into the pJL207

vector cut with the same restriction enzymes. The resulting plasmids (pHR081, pHR113, pHR086 and pHR114) were sequenced.

(v) pMLO59-derivative plasmids

The *paaR2-paaA2-parE2* locus was amplified on *E. coli* O157:H7 EDL933 genomic DNA using the following primers: *paaR2paaA2parE2* for and *paaR2paaA2parE2* rev. The PCR product was cloned into the TOPO-XL vector (Invitrogen) and sequenced. The recombinant TOPO-XL plasmid was digested with *Bam* HI and the locus-containing DNA fragment was ligated into the pMLO59 vector cut with the same restriction enzyme, generating the plasmid pHR068. pHR085 (pMLO-*paaA2-parE2*) was contructed by deleting *paaR2* from the pHR068 essentially as described in (Datsenko & Wanner, 2000). Briefly, the *cat* cassette was amplified from the pKD3 plasmid (Datsenko & Wanner, 2000) using primers Δ*paaR2* for and Δ*paaR2* rev. The PCR product was electroporated into a strain expressing the Red recombinase functions and containing the pHR068. Recombinant pMLO-*cat-paa2-parE2* plasmids were selected on LB chloramphenicol plates. The *cat* cassette was removed from the pMLO-*cat-paa2-parE2* plasmid using the pCP20 plasmid (Datsenko & Wanner, 2000), generating the plasmid pHR085.

β–galactosidase assays

The *E. coli* DJ624 strain harboring the plasmids pJL207 (control), pHR081 (P*R2*-lacZ), pHR113 (P*R2-paaR2-lacZ*), pHR086 (P*R2-paaR2-paaA2-lacZ*) or pHR114 (P*R2-paaR2-paaA2-parE2-lacZ*) was cultivated in LB broth at 37°C to mid-logarithmic phase. Samples were withdrawn to perform β-galactosidase assays as described in (Wilbaux et al., 2007). In the case of the *E. coli* DJ624 strain harbouring the plasmids pHR081 (P*R*2-lacZ) together with pKK223-3 (control), pHR082 (P*tac-paaR*2), pHR016 (P*tac-paaA2*), pHR023 (P*tac-paaA2-parE2*) or pHR097 (P*tac-paaR2-paaA2-parE2*) plasmids, expression from the P*tac* promoter was induced at mid-log by addition of IPTG

(100 µM) for 60 min prior β-galactosidase assays. The same procedure was applied for the CSH50λ*sfiA:lacZ* strain harbouring the plasmids pBAD33, pBAD33-$ccdB_F$, pHR033 (pBAD-*parE1*), pHR027 (pBAD-*parE2*), pHR034 (pBAD-*parE3*) or pHR035 (pBAD-$parE_{RK2}$) to measure the SOS induction, except that expression was induced by arabinose (1%) addition for 60 min prior β-galactosidase assays.

Subcellular localization of proteins

The *E. coli* MG1655 strain harbouring the plasmids pHR119 (pBAD-*parE2-gfp*), pHR073 (pBAD-*paaA2-gfp*) and pHR072 (pBAD-*gfp-paaA2*) were grown at 37°C in MM supplemented with chloramphenicol and glucose (0.4%) to mid-logarithmic phase. Cultures were then washed with MM and pellets resuspended in MM with chloramphenicol and arabinose (0.1%) for 60 min. The *E. coli* DJ624 strain harbouring the plasmids pHR119 (pBAD-*parE2-gfp*) with pKK223-3 (control), pHR016 (P*tac-paaA2*), pHR117 (P*tac-flag-paaA2*) or pHR122 (P*tac-paaA2-flag*) were grown in the same conditions except that after washing, pellets were resuspended in MM with ampicillin, chloramphenicol, arabinose (0.1%) and IPTG (100 µM). Two µl of cultures were placed on microscope slides layered with PBS 1% agarose pad. When indicated, samples were stained with DAPI by resuspending 100 µl of pelleted cells into 100 µl of PBS containing 5 µg of DAPI before microscopic examinations.

Co-immunoprecipitation assay

The *E. coli* DJ624 strain harbouring the plasmids pHR055 (pBAD33-*gfp mut2*-T7.tag) or pHR119 (pBAD-*parE2-gfp*) together with pKK223-3 (control) or pHR122 (P*tac-paaA2-flag*) were grown at 37°C in MM supplemented with chloramphenicol, ampicillin and glucose (0.4%) to mid-logarithmic phase. The cultures were then washed in MM and pellets resuspended in MM supplemented with chloramphenicol, ampicillin, arabinose (0.1%) and IPTG (100 µM) for 60 min. Three ml of cultures

were lyzed with the Lysis Buffer (FLAG-IPT-1 Sigma) as recommended by the manufacturer. One hundred µl of lyzed cells (whole cell lyzates) was withdrawn before immunoprecipitation (IP). The lyzed cells were then immunoprecipitated with anti-FLAG M2 Monoclonal antibodies (Sigma). Both whole cell lyzates and IP were separated on a SDS-PAGE (12 % acrylamide), transferred on nitrocellulose membrane, probed with anti-FLAG and monoclonal anti-GFP (Clone GSN24, Sigma), and with a seconday anti-Mouse IgG (Goat) HRP-labeled (Perkin Elmer). Signals were detected using ECL Western Blotting Kit (GE Healthcare).

Rescue experiment

The *E. coli* DJ624 strain harbouring the plasmids pBAD33 (control) or pHR027 (pBAD-*parE2*) with pWSK129 or pHR133 (P*lac-paaA2*) were grown in LB supplemented with 50 µg/ml kanamycin and 20 µg/ml of chloramphenicol at 37°C to an OD_{600nm} of 0.2. Cultures were diluted to an OD_{600nm} of 0.02 and arabinose (1%) was added with IPTG (2mM) or without. At indicated time, samples were plated on LB containing 0.4 % glucose, 50 µg/ml kanamycin, 20 µg/ml choramphenicol with IPTG (2mM) or without. Colony forming unit per ml were determined.

Post-segregational killing assay

The PSK assay using the pMLO59 vector and its derivatives was performed essentially as described in (Wilbaux et al., 2007). Briefly, *E. coli* strains containing pMLO59, pMLO-*paaR2-paaA2-parE2* (pHR068) or pMLO-*paaA2-parE2* (pHR085) plasmids were grown in LB with spectinomycin (100 µg/ml) at 30°C. Mid-log phase cultures were diluted in LB at 42°C and colony forming unit per ml were determined on LB and LB spectinomycin plates (100 µg/ml) at 30°C to determine viability and plasmid retention, respectively.

Half-life of PaaA2

E. coli MG1655, *lon::tet*, *clpP::cat*, *clpA::kan*, *clpX::kan*, *clpX::kan/clpA::tet* and Δ*lon clpP::cat* strains harbouring the pHR122 (P*tac-paaA2-flag*) plasmid were grown in logarithmic phase in LB medium at 37°C. Expression of *paaA2-flag* was induced for 120 min with IPTG (1mM) and at time zero (OD_{600} of 0.3-0.5), translation was blocked by the addition of chloramphenicol for MG1655, *lon::tet*, *clpA::kan*, *clpX::kan*, *clpX::kan*/*clpA::tet* and tetracycline for MG1655, *clpP::cat* and Δ*lon clpP::cat*. At indicated time, samples were withdrawn, harvested and resuspended in SDS-loading buffer. Equal amounts of total proteins for each strain were separated on a SDS-PAGE (15 % acrylamide), transferred on nitrocellulose membrane, probed with anti-FLAG M2 Monoclonal antibodies (Sigma), then with secondary anti-Mouse IgG (Goat) HRP-labeled (Perkin Elmer). Signals were detected using ECL Western Blotting Kit (GE Healthcare). Films were then scanned and band intensities were quantified with ImageJ software. Formula for determining half-life was obtained from the line fitting of the decay curves using Microsoft Excel.

Table 1. PaaA2 is unstable and degraded by ClpXP, ClpAP and Lon proteases

Strain	$t_{1/2}$ PaaA2-FLAG (min)
MG1655	6*
lon::tet	6
clpP::cat	28
clpA::kan	5
clpX::kan	10
clpX::kan clpA::tet	51
Δ*lon clpP::cat*	>120

* Blocking translation with chloramphenicol or tetracycline did not influence the half-life of PaaA2-FLAG

Table 2. Strains and Plasmids

Strain	Relevant Genotype or Description	Reference or Source
MG1655	Wild-type *E. coli* K-12	(Xiao *et al.*, 1991)
CSH50λ*sfiA::lacZ*	*ara* Δ(*lac-pro*) *strA thi* λ*sfiA::lacZ*	(Van Melderen *et al.*, 1994)
DJ624	MG1655 Δ*lac malP::lacI*^{q}	(Vanderpool & Gottesman, 2007)
DJ624 Δ *ara*	DJ624 Δ *ara*	our laboratory
lon::tet	MG1655 *lon::tet*	our laboratory
clpP::cat	MG1655 *clpP::cat*	our laboratory
clpA::kan	MG1655 *clpA::kan*	our laboratory
clpX::kan	MG1655 *clpX::kan*	our laboratory
clpX::kan clpA::tet	MG1655 *clpX::kan clpA::tet*	This work
Δ*lon clpP::cat*	MG1655 Δ *lon clpP::cat*	our laboratory
EDL933 O157:H7	Enterohemorrhagic	(Riley *et al.*, 1983)
133	EDL933 Δ*paaA1parE1::kan*	This work
136	EDL933 Δ*paaA2parE2::kan*	This work
139	EDL933 Δ$parD_{EDL933}$*parE3::kan*	This work

Plasmid	Relevant Genotype or Description	Reference or Source
pBAD33	P15A, Cam^{R}, pBAD promoter	(Guzman *et al.*, 1995)
pHR033	pBAD-*parE1*	This work
pHR027	pBAD-*parE2*	This work
pHR034	pBAD-*parE3*	This work
pHR035	pBAD-$parE_{RK2}$	This work
pHR054	pBAD-T7.tag-*gfp mut2*	This work
pHR055	pBAD-*gfp mut2*-T7.tag	This work
pHR119	pBAD-*parE2-gfp*	This work
pHR073	pBAD-*paaA2-gfp*	This work

1	pHR072	pBAD-*gfp-paaA2*	This work
2	pKK223-3	ColE1, Amp^R, P*tac* promoter	(Brosius & Holy, 1984)
3	pHR036	P*tac-paaA1*	This work
4	pHR016	P*tac-paaA2*	This work
5	pHR023	P*tac-paaA2-parE2*	This work
6	pHR037	P*tac-parD*$_{EDL933}$	This work
7	pHR038	P*tac-parD*$_{RK2}$	This work
8	pHR082	P*tac-paaR2*	This work
9	pHR097	P*tac-paaR2-paaA2-parE2*	This work
10	pHR117	P*tac-flag-paaA2*	This work
11	pHR122	P*tac-paaA2-flag*	This work
12	pWSK129	pSC101, Kan^R, P*lac* promoter	(Wang & Kushner, 1991)
13	pHR133	P*lac-paaA2*	This work
14	PJL207	P15A, Cam^R, *lacZ*	(Light & Molin, 1982)
15	pHR081	P*R2-lacZ*	This work
16	pHR113	P*R2-paaR2-lacZ*	This work
17	pHR086	P*R2-paaR2-paaA2-lacZ*	This work
18	pHR114	P*R2-paaR2-paaA2-parE2-lacZ*	This work
19	pMLO59	P15A ts derivative, $Spec^R$	M. Labocka
20	pHR068	pMLO-*paaR2-paaA2-parE2*	This work
21	pHR085	pMLO-*paaA2-parE2*	This work
22			

FIGURE LEGENDS

Figure 1. Genetic organization of the parE loci of E. coli O157:H7

The intergenic regions between each ORF (bp) are indicated. The accession numbers as well as the size (aa) of the predicted proteins are: NP_309096 (PaaR1, 133 aa), NP_309095 (PaaA1, 63 aa), NP_309094 (ParE1, 95 aa), NP_310307 (PaaR2, 144 aa), NP_310307 (PaaA2, 63 aa), NP_310308 (ParE2, 92 aa), NP_308488 ($ParD_{EDL933}$, 80 aa) and NP_308489 (ParE3, 93 aa).

Figure 2. ORFs encoded upstream of parE paralogs are functional antitoxins

(A) *E. coli* MG1655 strain harbouring the pBAD33, pBAD-*parE1*, pBAD-*parE2*, pBAD-*parE3* or pBAD-$parE_{RK2}$ plasmids with either pKK223-3, P*tac-paaA1*, P*tac-paaA2*, P*tac-*$parD_{EDL933}$ or P*tac-*$parD_{RK2}$ plasmids were streaked on MM supplemented with chloramphenicol, ampicillin and either glucose 0.2% (A1) or arabinose 1% (A2). (B) *E. coli* O157:H7 EDL933 (wt), Δ*paaA1-parE1::kan* (Δ1), Δ*paaA2-parE2::kan* (Δ2) and Δ$parD_{EDL933}$-*parE3::kan* (Δ3) strains containing the pBAD33, pBAD-*parE1*, pBAD-*parE2*, pBAD-*parE3* or pBAD-$parE_{RK2}$ plasmids were streaked on MM supplemented with chloramphenicol, and either glucose 0.2% (B1) or arabinose 1% (B2).

Figure 3. Ectopic overexpression of ParE2 is bactericidal

E. coli DJ624 Δ*ara* strain harbouring the pBAD33 and pWSK129 vectors (CTL plasmids, open circles) or pBAD-*parE2* and P*lac-paaA2* (PaaA2/ParE2, squares) were grown to mid-log at 37°C in LB medium containing arabinose (1%) with and without IPTG (+IPTG 2mM : filled squares, –IPTG: open squares). Samples were plated on LB plates containing glucose (0.4%) with or without IPTG (+IPTG 2mM: black lines, –IPTG: dotted lines). Values represented on the graph correspond to the average of data of 3 independent experiments.

Figure 4. PaaA2 neutralizes ParE2 toxicity by releasing it from the nucleoid through a physical interaction

(A) *E. coli* MG1655 strains harbouring the P*tac-paaA2-flag* plasmid with the pBAD-*gfp* (1) or pBAD-*parE2-gfp* (2) plasmids were grown and whole cell lysates (lysates) were prepared as described in Materials and Methods. PaaA2-FLAG was immunoprecipitated from both lysates using anti-FLAG antibodies (IP). Proteins from IP as well as from cell lysates were separated on SDS-PAGE, and revealed by Western blotting with monoclonal anti-FLAG and anti-GFP antibodies. *E. coli* MG1655 strains harbouring pBAD-*parE2-gfp* alone (B) or with the P*tac-paaA2-flag* (C), pBAD-*gfp-paaA2* (D1) and pBAD-*paaA2-gfp* (D2) were grown as described in Materials and Methods. Phase contrast and corresponding fluorescence images were overlayed. Scale bar, 2µm.

Figure 5. PaaR2 and the PaaA2/ParE2 complex regulate negatively expression of the paaR2-paaA2-parE2 system

(A) Sequence of the *paaR2-paaA2-parE2* upstream DNA region. The position of the predicted -35 (dark grey) and -10 (light grey) promoter sequences for P*R2* are underlined. (B) *E. coli* DJ624 strain harbouring the P*R2-lacZ* with pKK223-3, P*tac-paaR2*, P*tac-paaA2*, P*tac-paaA2-parE2* or P*tac-paaR2-paaA2-parE2* plasmids were grown and β-galactosidase assays were performed as described in Materials and Methods. Experiments were performed 3 times and promoter activities are expressed in Miller Units (Average ± SD). (C) *E. coli* DJ624 strain harbouring the pJL207-*lacZ*, P*R2-lacZ*, P*R2-paaR2-lacZ*, P*R2-paaR2-paaA2-lacZ* or P*R2-paaR2-paaA2-parE2-lacZ*) plasmids were grown and β-galactosidase assays were performed as described in Materials and Methods. Experiments were performed 3 times and promoter activities are expressed in Miller Units (Average ± SD).

Figure 6: Post-segregational killing mediated by paaR2-paaA2-parE2 is abolished in mutant proteases and requires the paaR2 transcriptional regulator

MG1655 (wt) and its derivatives *clpP* (*clpP::cat*), *clpA* (*clpA::kan*), *clpX* (*clpX::kan*) and *lon* (*lon::tet*) containing the pMLO-*paaR2-paaA2-parE2* and MG1655 containing the pMLO-*paaA2-parE2* with (wt+*paaA2*) and without P*tac-paaA2* (wt) were grown at 42°C and samples were plated on LB and LB spectinomycin plates for 180 min. Viability represents the number of viable counts of MG1655 and its derivatives/pMLO-*paaR2-paaA2-parE2* or MG1655/pMLO-*paaA2-parE2* on LB plates normalized to the number of viable counts of MG1655 and its derivatives/pMLO59 on LB plates. Plasmid retention represents the number of viable counts of MG1655 and its derivatives/pMLO-*paaR2-paaA2-parE2* or MG1655/pMLO-*paaA2-parE2* on LB spectinomycin plates normalized to the number of viable counts of MG1655 and its derivatives/pMLO59 on LB spectinomycin plates.

ACKNOWLEDGMENTS

We are grateful to Abram Aertsen and Urs Jenal for comments on the manuscript. We thank all members of the lab for exciting and constructive discussions, Susan Gottesman and Nadim Majdalani for providing ATP-dependent protease mutant strains and Khadija Wahni for excellent technical support. We thank Etienne Pays for the access to the fluorescence microscope. LVM was supported by research grants from FNRS (FRSM-3.4530.04), European Union (STREP CRAB, LSHM-CT-2005-019023), Fondation Van Buuren and Fonds Jean Brachet. DG is supported by the FRIA. RL was supported by research grants from OZR-VUB, VIB and FWO-Vlaanderen. YS acknowledges the receipt of an individual predoctoral fellowship from FWO-Vlaanderen.

REFERENCES

Afif, H., N. Allali, M. Couturier & L. Van Melderen (2001) The ratio between CcdA and CcdB modulates the transcriptional repression of the ccd poison-antidote system. *Mol Microbiol* **41:** 73-82.

Bahassi, E. M., M. H. O'Dea, N. Allali, J. Messens, M. Gellert & M. Couturier (1999) Interactions of CcdB with DNA gyrase. Inactivation of Gyra, poisoning of the gyrase-DNA complex, and the antidote action of CcdA. *J Biol Chem* **274:** 10936-10944.

Bernard, P. & M. Couturier (1992) Cell killing by the F plasmid CcdB protein involves poisoning of DNA-topoisomerase II complexes. *J Mol Biol* **226:** 735-745.

Bernard, P., K. E. Kezdy, L. Van Melderen, J. Steyaert, L. Wyns, M. L. Pato, P. N. Higgins & M. Couturier (1993) The F plasmid CcdB protein induces efficient ATP-dependent DNA cleavage by gyrase. *J Mol Biol* **234:** 534-541.

Brosius, J. & A. Holy (1984) Regulation of ribosomal RNA promoters with a synthetic lac operator. *Proc Natl Acad Sci U S A* **81:** 6929-6933.

Budde, P. P., B. M. Davis, J. Yuan & M. K. Waldor (2007) Characterization of a higBA toxin-antitoxin locus in Vibrio cholerae. *J Bacteriol* **189:** 491-500.

Cam, K., S. Bejar, D. Gil & J. P. Bouche (1988) Identification and sequence of gene dicB: translation of the division inhibitor from an in-phase internal start. *Nucleic Acids Res* **16:** 6327-6338.

Ceglowski, P., A. Boitsov, S. Chai & J. C. Alonso (1993) Analysis of the stabilization system of pSM19035-derived plasmid pBT233 in Bacillus subtilis. *Gene* **136:** 1-12.

Chaveroche, M. K., J. M. Ghigo & C. d'Enfert (2000) A rapid method for efficient gene replacement in the filamentous fungus Aspergillus nidulans. *Nucleic Acids Res* **28:** E97.

Chin, N. X. & H. C. Neu (1983) In vitro activity of enoxacin, a quinolone carboxylic acid, compared with those of norfloxacin, new beta-lactams, aminoglycosides, and trimethoprim. *Antimicrob Agents Chemother* **24:** 754-763.

Christensen, S. K., G. Maenhaut-Michel, N. Mine, S. Gottesman, K. Gerdes & L. Van Melderen (2004) Overproduction of the Lon protease triggers inhibition of translation in Escherichia coli: involvement of the yefM-yoeB toxin-antitoxin system. *Mol Microbiol* **51:** 1705-1717.

Christensen, S. K., K. Pedersen, F. G. Hansen & K. Gerdes (2003) Toxin-antitoxin loci as stress-response-elements: ChpAK/MazF and ChpBK cleave translated RNAs and are counteracted by tmRNA. *J Mol Biol* **332:** 809-819.

Christensen-Dalsgaard, M. & K. Gerdes (2006) Two higBA loci in the Vibrio cholerae superintegron encode mRNA cleaving enzymes and can stabilize plasmids. *Mol Microbiol* **62:** 397-411.

Critchlow, S. E., M. H. O'Dea, A. J. Howells, M. Couturier, M. Gellert & A. Maxwell (1997) The interaction of the F plasmid killer protein, CcdB, with DNA gyrase: induction of DNA cleavage and blocking of transcription. *J Mol Biol* **273:** 826-839.

Datsenko, K. A. & B. L. Wanner (2000) One-step inactivation of chromosomal genes in Escherichia coli K-12 using PCR products. *Proc Natl Acad Sci U S A* **97:** 6640-6645.

de la Hoz, A. B., S. Ayora, I. Sitkiewicz, S. Fernandez, R. Pankiewicz, J. C. Alonso & P. Ceglowski (2000) Plasmid copy-number control and better-than-random segregation genes of pSM19035 share a common regulator. *Proc Natl Acad Sci U S A* **97:** 728-733.

de la Hoz, A. B., F. Pratto, R. Misselwitz, C. Speck, W. Weihofen, K. Welfle, W. Saenger, H. Welfle & J. C. Alonso (2004) Recognition of DNA by omega protein from the broad-host range Streptococcus pyogenes plasmid pSM19035: analysis of binding to operator DNA with one to four heptad repeats. *Nucleic Acids Res* **32:** 3136-3147.

Ding, Z., Z. Zhao, S. J. Jakubowski, A. Krishnamohan, W. Margolin & P. J. Christie (2002) A novel cytology-based, two-hybrid screen for bacteria applied to protein-protein interaction studies of a type IV secretion system. *J Bacteriol* **184:** 5572-5582.

Dmowski, M., I. Sitkiewicz & P. Ceglowski (2006) Characterization of a novel partition system encoded by the delta and omega genes from the streptococcal plasmid pSM19035. *J Bacteriol* **188:** 4362-4372.

Eliopoulos, G. M., A. E. Moellering, E. Reiszner & R. C. Moellering, Jr. (1985) In vitro activities of the quinolone antimicrobial agents A-56619 and A-56620. *Antimicrob Agents Chemother* **28:** 514-520.

Fozo, E. M., K. S. Makarova, S. A. Shabalina, N. Yutin, E. V. Koonin & G. Storz Abundance of type I toxin-antitoxin systems in bacteria: searches for new candidates and discovery of novel families. *Nucleic Acids Res*.

Gerdes, K., S. K. Christensen & A. Lobner-Olesen (2005) Prokaryotic toxin-antitoxin stress response loci. *Nat Rev Microbiol* **3:** 371-382.

Gerdes, K., P. B. Rasmussen & S. Molin (1986) Unique type of plasmid maintenance function: postsegregational killing of plasmid-free cells. *Proc Natl Acad Sci U S A* **83:** 3116-3120.

Gotfredsen, M. & K. Gerdes (1998) The Escherichia coli relBE genes belong to a new toxin-antitoxin gene family. *Mol Microbiol* **29:** 1065-1076.

Guzman, L. M., D. Belin, M. J. Carson & J. Beckwith (1995) Tight regulation, modulation, and high-level expression by vectors containing the arabinose PBAD promoter. *J Bacteriol* **177:** 4121-4130.

Hooper, D. C. (2001) Mechanisms of action of antimicrobials: focus on fluoroquinolones. *Clin Infect Dis* **32 Suppl 1:** S9-S15.

Jaffe, A., T. Ogura & S. Hiraga (1985) Effects of the ccd function of the F plasmid on bacterial growth. *J Bacteriol* **163:** 841-849.

Jensen, R. B., E. Grohmann, H. Schwab, R. Diaz-Orejas & K. Gerdes (1995) Comparison of ccd of F, parDE of RP4, and parD of R1 using a novel conditional replication control system of plasmid R1. *Mol Microbiol* **17:** 211-220.

Jiang, Y., J. Pogliano, D. R. Helinski & I. Konieczny (2002) ParE toxin encoded by the broad-host-range plasmid RK2 is an inhibitor of Escherichia coli gyrase. *Mol Microbiol* **44:** 971-979.

Jorgensen, M. G., D. P. Pandey, M. Jaskolska & K. Gerdes (2009) HicA of Escherichia coli defines a novel family of translation-independent mRNA interferases in bacteria and archaea. *J Bacteriol* **191:** 1191-1199.

Light, J. & S. Molin (1982) Expression of a copy number control gene (copB) of plasmid R1 is constitutive and growth rate dependent. *J Bacteriol* **151:** 1129-1135.

Lima-Mendez, G., J. Van Helden, A. Toussaint & R. Leplae (2008) Prophinder: a computational tool for prophage prediction in prokaryotic genomes. *Bioinformatics* **24:** 863-865.

Liu, M., Y. Zhang, M. Inouye & N. A. Woychik (2008) Bacterial addiction module toxin Doc inhibits translation elongation through its association with the 30S ribosomal subunit. *Proc Natl Acad Sci U S A* **105:** 5885-5890.

Magnuson, R. & M. B. Yarmolinsky (1998) Corepression of the P1 addiction operon by Phd and Doc. *J Bacteriol* **180:** 6342-6351.

Magnuson, R. D. (2007) Hypothetical functions of toxin-antitoxin systems. *J Bacteriol* **189:** 6089-6092.

Makarova, K. S., Y. I. Wolf & E. V. Koonin (2009) Comprehensive comparative-genomic analysis of type 2 toxin-antitoxin systems and related mobile stress response systems in prokaryotes. *Biol Direct* **4:** 19.

Monti, M. C., A. M. Hernandez-Arriaga, M. B. Kamphuis, J. Lopez-Villarejo, A. J. Heck, R. Boelens, R. Diaz-Orejas & R. H. van den Heuvel (2007) Interactions of Kid-Kis toxin-antitoxin complexes with the parD operator-promoter region of plasmid R1 are piloted by the Kis antitoxin and tuned by the stoichiometry of Kid-Kis oligomers. *Nucleic Acids Res* **35:** 1737-1749.

Pandey, D. P. & K. Gerdes (2005) Toxin-antitoxin loci are highly abundant in free-living but lost from host-associated prokaryotes. *Nucleic Acids Res* **33:** 966-976.

Pedersen, K., A. V. Zavialov, M. Y. Pavlov, J. Elf, K. Gerdes & M. Ehrenberg (2003) The bacterial toxin RelE displays codon-specific cleavage of mRNAs in the ribosomal A site. *Cell* **112:** 131-140.

Riley, L. W., R. S. Remis, S. D. Helgerson, H. B. McGee, J. G. Wells, B. R. Davis, R. J. Hebert, E. S. Olcott, L. M. Johnson, N. T. Hargrett, P. A. Blake & M. L. Cohen (1983) Hemorrhagic colitis associated with a rare Escherichia coli serotype. *N Engl J Med* **308:** 681-685.

Roberts, R. C. & D. R. Helinski (1992) Definition of a minimal plasmid stabilization system from the broad-host-range plasmid RK2. *J Bacteriol* **174:** 8119-8132.

Roberts, R. C., A. R. Strom & D. R. Helinski (1994) The parDE operon of the broad-host-range plasmid RK2 specifies growth inhibition associated with plasmid loss. *J Mol Biol* **237:** 35-51.

Rowe-Magnus, D. A., A. M. Guerout, L. Biskri, P. Bouige & D. Mazel (2003) Comparative analysis of superintegrons: engineering extensive genetic diversity in the Vibrionaceae. *Genome Res* **13:** 428-442.

Sat, B., R. Hazan, T. Fisher, H. Khaner, G. Glaser & H. Engelberg-Kulka (2001) Programmed cell death in Escherichia coli: some antibiotics can trigger mazEF lethality. *J Bacteriol* **183:** 2041-2045.

Schmidt, O., V. J. Schuenemann, N. J. Hand, T. J. Silhavy, J. Martin, A. N. Lupas & S. Djuranovic (2007) prlF and yhaV encode a new toxin-antitoxin system in Escherichia coli. *J Mol Biol* **372:** 894-905.

Schumacher, M. A., K. M. Piro, W. Xu, S. Hansen, K. Lewis & R. G. Brennan (2009) Molecular mechanisms of HipA-mediated multidrug tolerance and its neutralization by HipB. *Science* **323:** 396-401.

Sevin, E. W. & F. Barloy-Hubler (2007) RASTA-Bacteria: a web-based tool for identifying toxin-antitoxin loci in prokaryotes. *Genome Biol* **8:** R155.

Smith, A. S. & D. E. Rawlings (1997) The poison-antidote stability system of the broad-host-range Thiobacillus ferrooxidans plasmid pTF-FC2. *Mol Microbiol* **26:** 961-970.

Suzuki, M., J. Zhang, M. Liu, N. A. Woychik & M. Inouye (2005) Single protein production in living cells facilitated by an mRNA interferase. *Mol Cell* **18:** 253-261.

Szekeres, S., M. Dauti, C. Wilde, D. Mazel & D. A. Rowe-Magnus (2007) Chromosomal toxin-antitoxin loci can diminish large-scale genome reductions in the absence of selection. *Mol Microbiol* **63:** 1588-1605.

Tsilibaris, V., G. Maenhaut-Michel, N. Mine & L. Van Melderen (2007) What is the benefit to Escherichia coli of having multiple toxin-antitoxin systems in its genome? *J Bacteriol* **189:** 6101-6108.

Van Melderen, L. (2002) Molecular interactions of the CcdB poison with its bacterial target, the DNA gyrase. *Int J Med Microbiol* **291:** 537-544.

Van Melderen, L., P. Bernard & M. Couturier (1994) Lon-dependent proteolysis of CcdA is the key control for activation of CcdB in plasmid-free segregant bacteria. *Mol Microbiol* **11:** 1151-1157.

Van Melderen, L. & M. Saavedra De Bast (2009) Bacterial toxin-antitoxin systems: more than selfish entities? *PLoS Genet* **5:** e1000437.

Vanderpool, C. K. & S. Gottesman (2007) The novel transcription factor SgrR coordinates the response to glucose-phosphate stress. *J Bacteriol* **189:** 2238-2248.

Wang, R. F. & S. R. Kushner (1991) Construction of versatile low-copy-number vectors for cloning, sequencing and gene expression in Escherichia coli. *Gene* **100:** 195-199.

Weihofen, W. A., A. Cicek, F. Pratto, J. C. Alonso & W. Saenger (2006) Structures of omega repressors bound to direct and inverted DNA repeats explain modulation of transcription. *Nucleic Acids Res* **34:** 1450-1458.

Wilbaux, M., N. Mine, A. M. Guerout, D. Mazel & L. Van Melderen (2007) Functional interactions between coexisting toxin-antitoxin systems of the ccd family in Escherichia coli O157:H7. *J Bacteriol* **189:** 2712-2719.

Winther, K. S. & K. Gerdes (2009) Ectopic production of VapCs from Enterobacteria inhibits translation and trans-activates YoeB mRNA interferase. *Mol Microbiol* **72:** 918-930.

Wozniak, R. A. & M. K. Waldor (2009) A toxin-antitoxin system promotes the maintenance of an integrative conjugative element. *PLoS Genet* **5:** e1000439.

Xiao, H., M. Kalman, K. Ikehara, S. Zemel, G. Glaser & M. Cashel (1991) Residual guanosine 3',5'-bispyrophosphate synthetic activity of relA null mutants can be eliminated by spoT null mutations. *J Biol Chem* **266:** 5980-5990.

Zeiler, H. J. (1985) Evaluation of the in vitro bactericidal action of ciprofloxacin on cells of Escherichia coli in the logarithmic and stationary phases of growth. *Antimicrob Agents Chemother* **28:** 524-527.

Zielenkiewicz, U. & P. Ceglowski (2005) The toxin-antitoxin system of the streptococcal plasmid pSM19035. *J Bacteriol* **187:** 6094-6105.

Figure 1

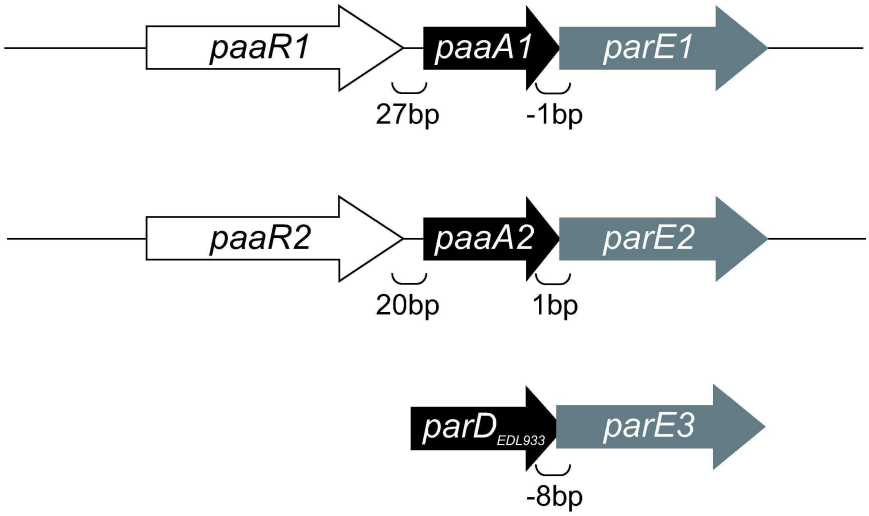

123x87mm (600 x 600 DPI)

Figure 2

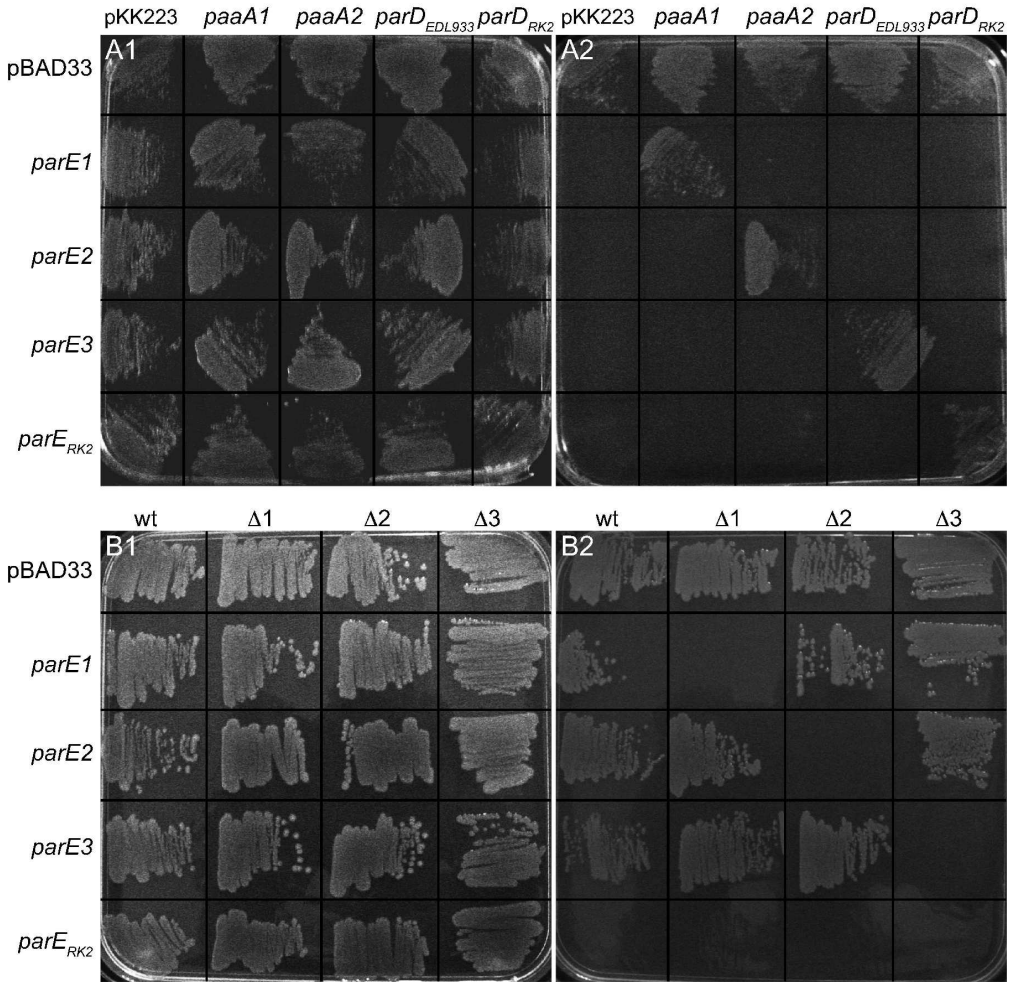

153x169mm (600 x 600 DPI)

Figure 3

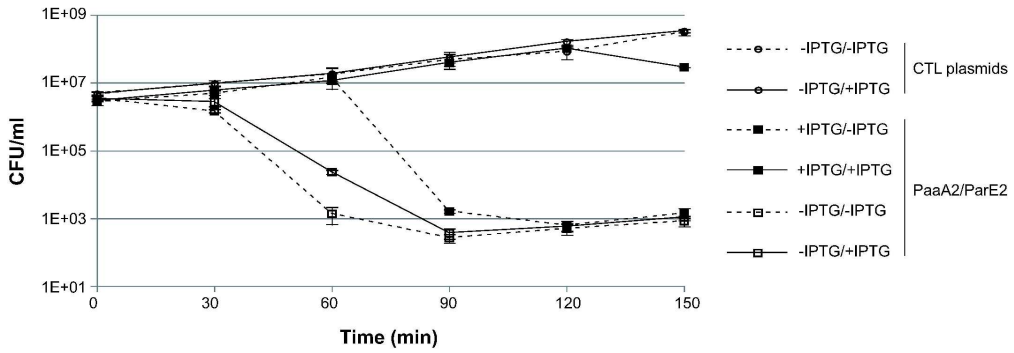

180x89mm (600 x 600 DPI)

Figure 4

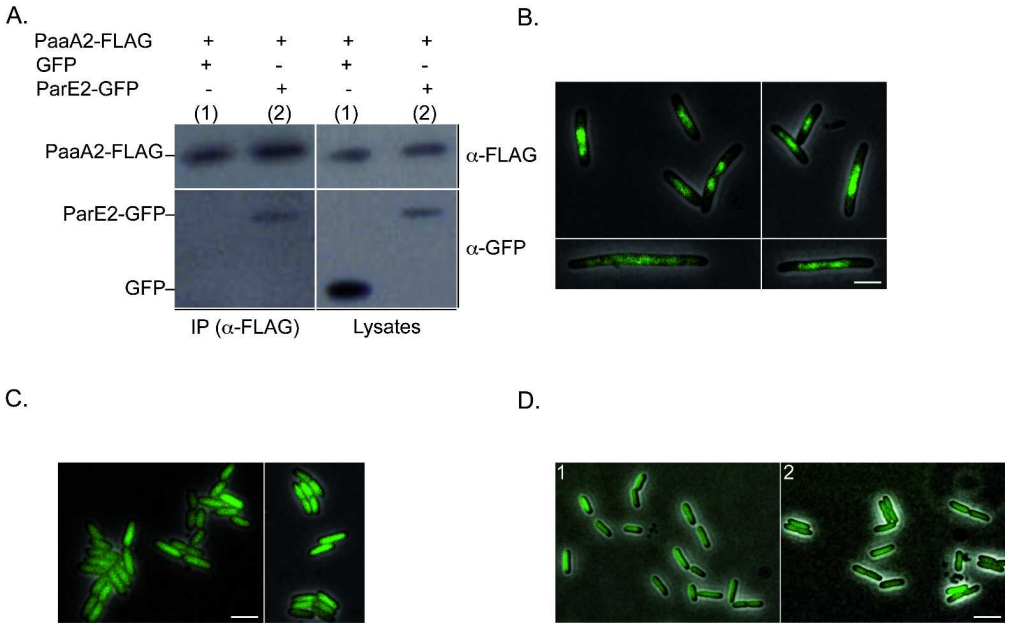

177x131mm (450 x 450 DPI)

Figure 5

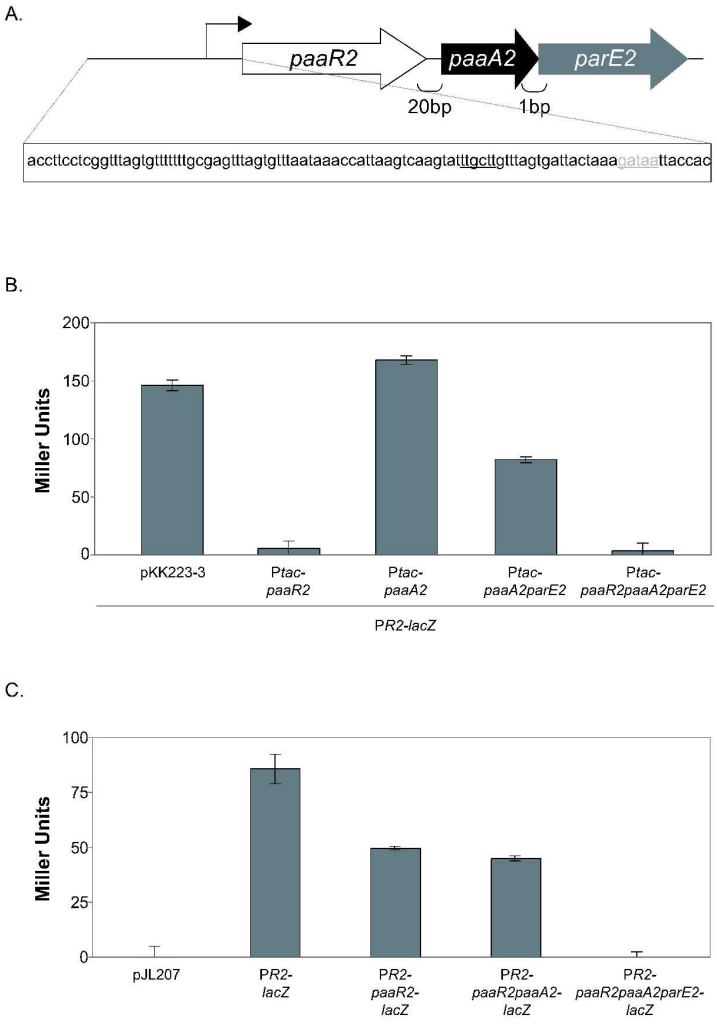

156x258mm (600 x 600 DPI)

Figure 6

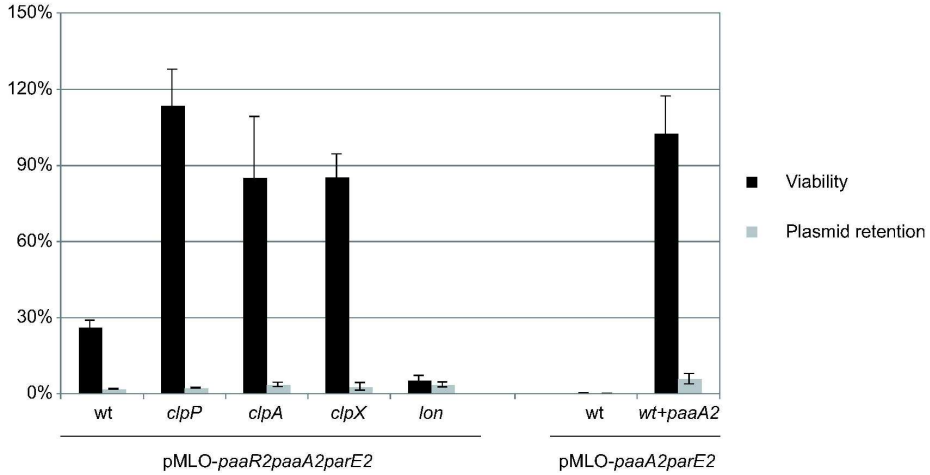

155x88mm (600 x 600 DPI)